Thermodynamic Interpretation of the Meyer-Neldel Rule Explains Temperature Dependence of Ion Diffusion in Silicate Glass

N. Takamure,[1,2,4,*] X. Sun,[1,†] T. Nagata,[3,‡] A. Ho-Baillie,[1,§] N. Fukata,[2,4,‖] and D. R. McKenzie[1,¶]

[1]School of Physics, University of Sydney, Sydney, New South Wales 2006, Australia
[2]Graduate School of Pure and Applied Sciences, University of Tsukuba, Tsukuba, Ibaraki 305-8573, Japan
[3]Research Center for Functional Materials, National Institute for Materials Science (NIMS), 1-1Namiki, Tsukuba 305-0044, Japan
[4]International Center for Materials for Nanoarchitectonics (MANA), National Institute for Materials Science (NIMS), 1-1Namiki, Tsukuba 305-0044, Japan

(Received 2 June 2022; accepted 30 September 2022; published 21 October 2022)

We study the temperature-dependent diffusion of many types of metal and semimetal ions in soda-lime glass using thermal relaxation ion spectroscopy, a technique that provides an electrical readout of thermally activated diffusion of charge carriers driven by built-in concentration gradients and electric fields. We measure the temperature of the onset of the motion, relevant to the long term storage of radioactive elements. We demonstrate the unique behavior of silver in soda-lime glass, enabling a thermal battery with rapid discharge of stored energy above a threshold temperature. We show that the Meyer-Neldel rule applies when comparisons of temperature-dependent diffusion rates are made between related measurements on one sample or between the same measurements on related samples. The results support a thermodynamic interpretation of the Meyer-Neldel rule as an enthalpy-entropy correlation where the Meyer-Neldel temperature (T_{MN}) is the temperature that enables liquidlike, barrier-free motion of the ions, with an upper limit set by the melting point of the host medium. This interpretation explains the observed reduction in T_{MN} by built-in electric fields in depletion layers and why the upper limit for T_{MN} for all ions is set by the glass transition temperature.

DOI: 10.1103/PhysRevLett.129.175901

Silicate glasses have been known since antiquity, with many uses relying on the presence of dopant elements. The dopants are usually positive ions held in sites associated with negatively charged nonbridging oxygen atoms of the silicate backbone. Modern applications rely on controlling the diffusion of ions in glass, including in-glass optoelectronics [1,2], device encapsulation [3,4], and long-term storage of radioactive waste [5–8]. In these applications, a knowledge of the temperature dependence of the mobility and diffusivity of dopants is essential [9]. It is widely observed that glass, polymers [10], and liquids [11] have a diffusion rate R with Arrhenius temperature dependence:

$$R = R_0 e^{-\Delta E_A/kT}, \tag{1}$$

where k is the Boltzmann constant. The quantity ΔE_A is referred to as the *activation energy* of the process and the prefactor R_0 as an *attempt frequency*. Eyring reaction rate theory, when applied to diffusion, proposes the existence of a transition state having an energy barrier relative to the initial state that must be overcome for the reaction to proceed. The Arrhenius relation (1) follows from Boltzmann statistics if ΔE_A is considered as the value of the energy barrier. The diffusion processes we are concerned with here occur at defined pressure and temperature conditions so that an energy difference between two configurations (e.g., the initial state and the transition state in Eyring theory) is correctly interpreted as a Gibbs free energy ΔG_A having enthalpic and entropic components:

$$\Delta G_A = \Delta H_A - T\Delta S_A\,, \tag{2}$$

where ΔH_A and ΔS_A are the enthalpy and entropy differences between the states. Such an interpretation relies on the thermodynamic functions G, H, and S retaining their meanings for the nanoscale system consisting of a diffusing ion and its surroundings. Substituting ΔG_A from Eq. (2) into Eq. (1) gives

$$R = a e^{\Delta S_A/k} e^{-\Delta H_A/kT}. \tag{3}$$

The prefactor R_0 in Eq. (1) becomes $a e^{\Delta S_A/k}$, dependent on the entropic component, where a is a constant scale factor.

When measurements are made of diffusion rate as a function of temperature on a set of related samples with small variations in fabrication or measurement conditions the Meyer-Neldel rule (MNR) [12,13] is widely observed as an enthalpy-entropy correlation:

$$\Delta S_A = kb\Delta H_A\,, \tag{4}$$

where b is constant. The need for a better understanding of the MNR is underlined by recent work where it has been

proposed as a guiding principle for designing fast ionic conductors [14]. Here, we apply the thermodynamic interpretation of the MNR as an enthalpy-entropy correlation [15] and explore its consequences for soda-lime glass. Combining Eqs. (3) and (4) and defining a Meyer-Neldel temperature by $T_{\mathrm{MN}} = 1/kb$, the diffusion rate temperature dependence is described by only two properties of the sample, T_{MN} and ΔH_A:

$$R = ae^{-\Delta H_A[(1/kT)-(1/kT_{\mathrm{MN}})]}. \tag{5}$$

For measurements of diffusion rate as a function of temperature that have different ΔH_A but the same T_{MN}, the MNR leads to an intersection point at T_{MN}, which leads to its alternative name, the *isokinetic temperature*. Dienes [16] gave a simple thermodynamic argument that relates T_{MN} to the local melting or disordering temperature where the rapid movement of the diffusing species occurs without a Gibbs free energy barrier. From Eq. (2), the Gibbs free energy barrier vanishes when the entropic contribution cancels the enthalpic contribution at T_{MN} so that

$$\Delta H_A = T_{\mathrm{MN}}\Delta S_A. \tag{6}$$

We now explore whether the hypothesis of Dienes could help explain the MNR correlation by giving meaning to T_{MN} for ion diffusion in soda-lime glass. A consequence of Dienes' hypothesis is that the value of T_{MN} should be related to the glass transition temperature, defined as the temperature above which the movement (in thermal equilibrium) of a diffusing ion to a new site is more probable than its return to its original site. Thermodynamics then asserts that the Gibbs free energy of the initial and transition states should be equal as the two states coexist at the same temperature and pressure. It is expected that an upper limit of T_{MN} in soda-lime glass for all diffusing ions would be set by the glass transition or softening temperature of the glass which enables dopant ions to become mobile in a viscous medium. Tracer diffusion [17] has revealed a sudden change in the activation energy for sodium and calcium ion diffusion in soda-lime glass at a temperature just below the glass transition temperature and shows that the rate of sodium diffusion below the glass transition temperature is 6 orders greater than for calcium diffusion, which is in turn much greater than the diffusion rate of the network former Si. Note that the diffusion rate in molten glass obeys Eq. (1), but the activation energy differs from that of the supercooled liquid (the glassy state). The Arrhenius temperature dependence of the liquid state contrasts with the $\sqrt{T}$ dependence of diffusion in ideal gases, because of the presence of local order that temporarily holds diffusing atoms in liquids in a "local cage" [18].

In this Letter, the thermodynamic interpretation of the MNR is facilitated by a convenient method for measurement of the temperature dependence of ion diffusion [19].

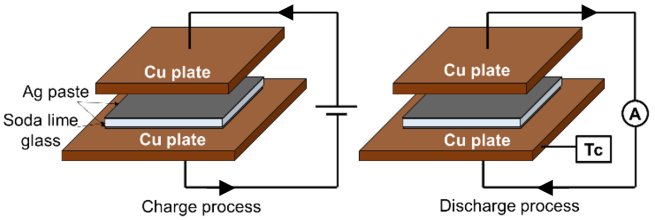

FIG. 1. (left) ions (Ag shown) are diffused into glass with electric field assistance using Cu plates in contact with electrodes applied directly on the glass. In TRIS (right) the spontaneous current is measured (arrow denotes positive) while the sample is reheated during a temperature ramp, retaining the anode side upward.

TRIS (thermal relaxation ion spectroscopy) is related to thermally stimulated depolarization current [20–22] for dielectric relaxation and deep level transient spectroscopy [23–25] for studying traps in semiconductors. Shockley related the velocity of a charged particle drifting between two electrodes to the current in a wire connecting the electrodes [26]. We used thermal diffusion with electric field assistance to insert a wide range of ions between 200 and 300 °C. A glass plate was placed between electrodes and voltage applied during baking, causing in-diffusion of metal ions from the anode. TRIS was then carried out by measuring (Keithley DMM7510) the current I_{SC} in a closed external circuit capacitively coupled to the sample subjected to a constant temperature ramp. TRIS is a useful advance for diffusion measurements as alternative methods (e.g., tracer diffusion [27]) are comparatively laborious. The setup is shown in Fig. 1.

To validate the TRIS method for diffusion studies, it is necessary to show that a single diffusion coefficient applies in the presence of concentration gradients as well as electric depolarization fields. When the temperature is elevated, ions move under the joint influence of concentration gradients and electric fields. Considering the diffusion as a 1D problem, the flux of ions of type i, j_i, is given by the sum of terms corresponding to Fick's law and the microscopic Ohm's law:

$$j_i(x) = -D_i\frac{\partial C_i}{\partial x} + \mu_i C_i E(x), \tag{7}$$

where C_i is the volume concentration of ions of type i, and the diffusion coefficient D_i is temperature dependent and related to the drift mobility μ_i in an electric field $E(x)$ by the Einstein-Smoluchowski-Sutherland equation [28]:

$$D_i = \frac{\mu_i kT}{q}, \tag{8}$$

where q is the charge. Doremus confirmed Eq. (8) applies to ion diffusion in soda-lime glass [27]. Substituting Eq. (8) in Eq. (7) we find the Nernst-Planck equation applies [29]:

$$j_i(x) = -D_i\left(\frac{\partial C_i}{\partial x} - \frac{q}{kT}C_i E(x)\right). \quad (9)$$

This equation has been used successfully for modeling the diffusion of ions in glass under the influence of electric fields [30]. Writing the diffusion coefficient in the activated form [Eq. (1)] we find for the ion flux:

$$j_i(x) = -D_{i0}\left(\frac{\partial C_i}{\partial x} - \frac{q}{kT}C_i E(x)\right)e^{-\Delta E_A/kT}. \quad (10)$$

From Shockley, the flux of ions at x contributes an amount $qj_i(x)$ to I_{sc} which is temperature activated through the diffusion coefficient, with the exponential activation term multiplied by a prefactor dependent on the concentration gradients and fields. The field-dependent term is only weakly temperature dependent. Therefore, activated behavior of the ion flux in Eq. (10) and hence the TRIS current, should apply.

Yelon, Movaghar, and Crandall derived a multiexcitation entropy theory for the MNR [31,32] in which the entropic contribution is described in terms of the summation of multiple small contributions from vibrational quanta. Multiexcitation entropy theory has recently been applied to diffusion in lithium solid-state electrolytes [33]. This microscopic theory has the potential to provide a mechanistic nanoscale explanation of the enthalpy-entropy correlation.

The first example of the MNR in soda-lime glass we discuss is a change in the activation energy of the low voltage conductivity at 1 V, of a single sample measured at various frequencies at a range of fixed temperatures, to create a set of temperature dependent measurements. In this case, the scale factor a is constant. The results [Fig. 2(a)] show that the activation energy obeys Eq. (5) with a T_{MN} of $480 \pm 20\,°C$, comparable to, but lower than the glass transition temperature (577 °C) [17], supporting the interpretation of T_{MN} of Dienes. The results of Fig. 2(b) demonstrate compliance with the MNR, with the T_{MN} of $480 \pm 10\,°C$, as for Fig. 2(a).

Silver enrichment of soda-lime glass by in-diffusion is used to create planar optical waveguides [1,2]. In a second type of experiment, we carried out electric field assisted diffusion of Ag by applying 200 V to silver electrodes pasted onto a 2 mm thick soda-lime glass plate at 300 °C for 20 min, to enrich the anodic side with silver. The low voltage conductivity of the sample was measured using the same conditions as the undoped sample. The results [Fig. 2(c)] obey Eq. (5) with a T_{MN} of $450 \pm 10\,°C$, in agreement with the T_{MN} obtained from the slope of Fig. 2(d). This lowering of T_{MN} relative to the undoped sample is likely to be related to silver, since in many silver-containing glasses the glass transition temperature is lowered relative to the undoped glass by up to 100 °C [34]. Alternatively, the presence of an electric field in the sample may also lower the glass transition temperature (see below). In either case, the results support our proposed link between T_{MN} and the glass transition temperature.

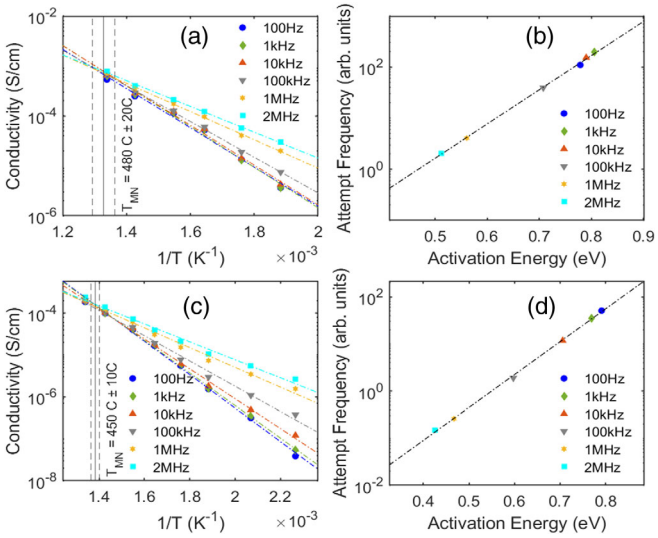

FIG. 2. (a) Measured low voltage conductivity at various frequencies for undoped soda lime glass as a function of inverse temperature, showing an intersection at a T_{MN} of $480 \pm 20\,°C$. (b) The attempt frequency as a function of activation energy for (a) shows a slope corresponding to a T_{MN} of $480 \pm 10\,°C$. (c) The low voltage conductivity as in (a) for soda-lime glass prediffused with Ag (200 V, 300 °C, 20 min.), showing intersection at a T_{MN} of $450 \pm 10\,°C$. (d) The attempt frequency as a function of activation energy for (c) giving a T_{MN} of $450 \pm 10\,°C$.

Ions of metals and semimetals were diffused into soda-lime glass under the same conditions (1500 V,

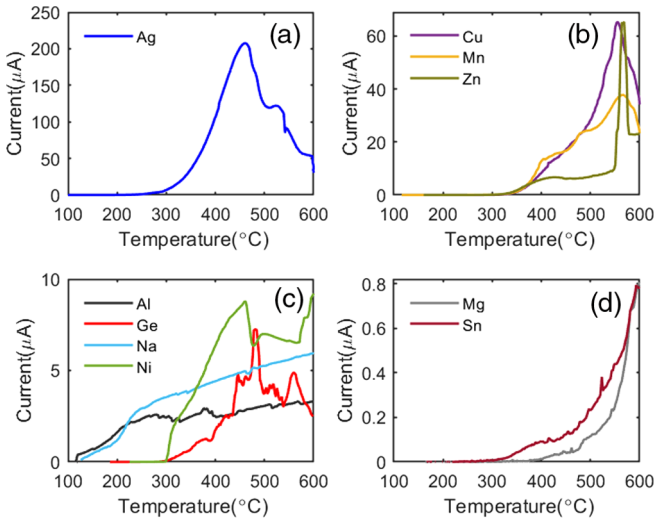

FIG. 3. The current generated as a function of temperature in TRIS for glass prediffused with various dopant ions using electric field assistance. (a) Ag, (b) Cu, Mn, and Zn, (c) Al, Ge, Na, and Ni, and (d) Mg and Sn. Na represents pure soda-lime glass having the same electric field treatment prior to measurement.

TABLE I. The temperature range in celsius for the onset of ion diffusion determined from TRIS for the various dopants shown in Fig. 3. The activation energy ΔE_A and attempt frequency R_0 of Eq. (1) for each ion species and the correlation coefficient R^2 from the activation plots [35] are also shown. Na refers to undoped soda-lime glass.

Element	Na	Ag	Al	Cu	Ge	Mg	Mn	Ni	Sn	Zn
Temp range (°C)	194–232	182–370	154–221	301–381	272–323	354–446	300–402	323–417	319–360	287–356
ΔE_A (eV)	0.51	0.99	0.30	1.92	2.24	1.25	1.58	0.44	1.16	1.71
R_0 (Hz)	3.3×10^5	3.7×10^9	2766.8	3.6×10^{15}	3.5×10^{18}	3.0×10^{18}	8.8×10^{12}	13351	1.0×10^8	1.1×10^{14}
R^2	0.9949	0.999	0.9965	0.9962	0.9945	0.9541	0.9968	0.9979	0.9841	0.9962

200 ~ 240 °C, 10 min). Results (current as a function of temperature) are shown in Fig. 3.

Table I shows the temperature range for the first detectable diffusion for each ion. The current at this temperature range obeys the Arrhenius equation [35]. The Mg ion begins to move at 354 °C, the highest temperature of all dopants, while the lowest temperature is shown by Al and Ag. The activation energy (activation enthalpy) covers a range of almost 2 eV while the attempt frequency covers 14 orders of magnitude because of the Meyer-Neldel correlation. We attribute the large variations in activation energy to the wide range of different dopant sizes and chemistries. When the enthalpy difference between the initial and final states (the heat released when the ion moves from the transition to the final state) changes, the attempt frequency also changes exponentially due to the Meyer-Neldel enthalpy-entropy correlation.

The Meyer-Neldel plot in Fig. 4 shows that the ratio of attempt frequency to activation energy for all ions is distributed around a single line with a T_{MN} of 393 ± 50 °C.

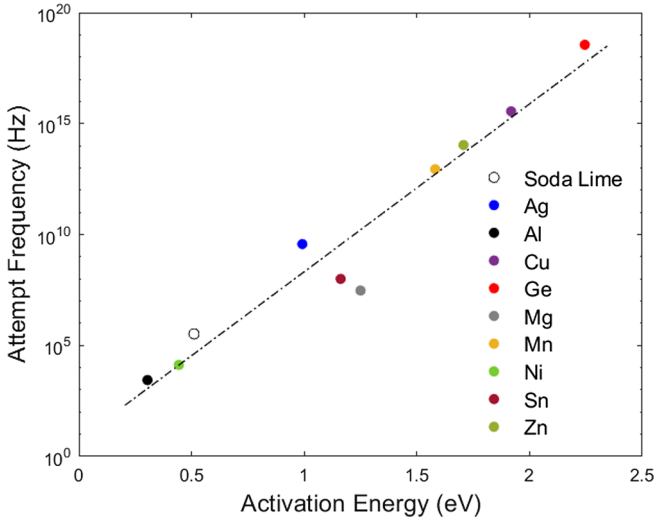

FIG. 4. Meyer-Neldel plot of attempt frequency against activation energy for soda-lime glass pre-diffused with Ag, Al, Cu, Ge, Mg, Mn, Ni, Sn, and Zn ions using electric field assistance. Undoped soda-lime glass subjected to an electric field prior to measurement is also shown for reference. The fitted line provides a T_{MN} of 393 ± 50 °C.

This T_{MN} is lower than the temperature obtained for Ag doped and undoped soda-lime glass from Fig. 2 and may be attributed to dopant metals lowering the glass transition temperature, and to the presence of electric fields known to induce softening in soda-lime glass [40]. All samples with prior electric field application showed lower T_{MN} than as-received soda-lime glass (Fig. 2).

The depletion layers formed by the electric field application are filled by ions during TRIS. Above T_{MN}, ion motion continues in a barrier-free manner limited by viscosity and varies from one ion to another [35]. Some ions (e.g., Ag) show a decreasing current while others (e.g., Mg, Sn, Ni) show a current still increasing up to 600 °C.

The Ag-doped sample was exceptional in generating the largest TRIS current. To examine the mechanism, the distribution of silver and sodium are shown in cross section in Figs. 5(a) and 5(b), obtained using energy dispersive analysis of x rays in a scanning electron microscope

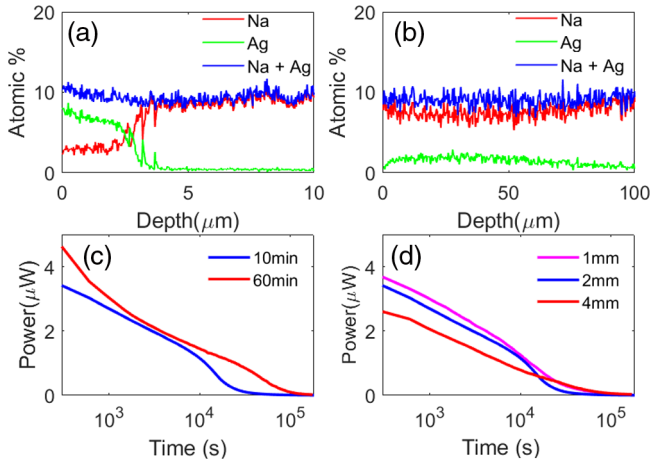

FIG. 5. (a) The distribution of Na, Ag, and their sum (Na + Ag) in soda-lime glass diffused with Ag using 200 V dc for 60 min. The surface layer is strongly enriched in Ag and the subsurface is depleted in Na. (b) After TRIS, Ag has diffused further into the glass, Na has returned toward the surface, and the depletion layer has been removed. (c) Discharge power as a function of time at 425 °C for an Ag glass "battery" using 2 mm thick glass with charging times of 10 and 60 min, respectively, at 1500 V. (d) Discharge power as in (c) for a 10 min charging time and three different glass thicknesses.

(Phenom XL). The silver ions entering the surface during the charging process do not fill all the sites vacated by sodium which moves toward the cathode, creating a depletion layer and a built-in electric field. After discharging, Fig. 5(b) shows that both Ag and Na ions become more evenly distributed. The sodium ions return to fill the depletion layer, contributing to the current in the external circuit. The inward diffusion of silver gives rise to a current that opposes the contribution from sodium. The external current may also have a contribution from electrons moving inward to neutralize Ag ions into electrically neutral nanoparticles, as previously observed [19]. Note that the silver behavior is essential to the production of large external currents, since all other ions only deliver small currents [Fig. 3(c)].

A potential application of silver diffused glass is a thermal "battery" where stored energy is delivered when the temperature rises above a threshold. To demonstrate power delivery, the current was discharged into a 46.9 kΩ load at a constant temperature of 425 °C. The peak discharge power decreased almost exponentially with time, increased with longer charging time [Fig. 5(c)] and decreased with increasing glass thickness [Fig. 5(d)]. The latter effect is consistent with Shockley's prediction [26].

The T_{MN} values of ion diffusion in soda-lime glass from this study are compared with some available values in the literature for ionic conduction in glasses of all types in Supplemental Material [35]. The MNR has been observed in cases of solid-state diffusion in crystalline semiconductors [41,42] and metallic glasses [43–47]. For diffusion in glassy metal alloys, T_{MN} is smaller than for crystalline alloys [48]. These observations, together with ours, support the idea that the melting of the host structure places an upper limit on the Meyer-Neldel temperature for ion diffusion. Note that electronic "hopping" conduction in semiconductor glasses also obeys the MNR [49].

In summary, this Letter has shown that TRIS conveniently measures the diffusion rate of ions introduced into soda-lime glass and that the Meyer-Neldel rule is well obeyed for all ions studied. Silver diffused glass has an exceptionally large energy storage in depletion layers and has been found to form a thermal battery. The application of TRIS may assist the design of new types of solid-state power source that use depletion layers and charge carrier diffusion as well as in finding hosts for stable storage of radioactive ions. Our findings support a classical thermodynamic interpretation of the Meyer-Neldel rule, originating from Dienes. The thermodynamic theory provides a satisfactory explanation of why the Meyer-Neldel temperature of all ions falls in a range below the glass transition temperature. The Meyer-Neldel temperature is interpreted as the temperature where rapid, barrier-free diffusion occurs because of local "melting" of the dopant ion substructure with an upper limit set by the melting of the backbone of the host medium. Further refinement of the theory will require the derivation of the enthalpy-entropy correlation from the atomic scale dynamics.

The Australian Research Council is acknowledged for financial support through the award of Discovery Project No. DP170102086 and Linkage Project No. LP160101322.

*noboru.takamure@sydney.edu.au
†xsun8303@uni.sydney.edu.au
‡nagata.takahiro@nims.go.jp
§anita.ho-baillie@sydney.edu.au
‖fukata.naoki@nims.go.jp
¶david.mckenzie@sydney.edu.au

[1] M. C. Ö. Yanık, M. S. Y. Öztürk, T. Yıldız, E. D. Kaçar, A. İyiel, B. İzmirlioğlu, and E. Günay, J. Non-Cryst. Solids **493**, 1 (2018).
[2] J.-E. Broquin and S. Honkanen, Appl. Sci. **11**, 4472 (2021).
[3] K. M. Knowles and A. T. J. van Helvoort, Int. Mater. Rev. **51**, 5273 (2013).
[4] L. Granados, R. Morena, N. Takamure, T. Suga, S. Huang, D. R. McKenzie, and A. Ho-Baillie, Mater. Today **47**, 131 (2021).
[5] B. Grambow, Elements **2**, 357 (2006).
[6] O. van Kessel, H. H. Brongersma, J. G. A. Hölscher, R. G. van Welzenis, E. G. F. Sengers, and F. J. J. G. Janssen, NIM-B **64**, 1593 (1992).
[7] J. D. Vienna, J. V. Ryan, S. Gin, and Y. Inagaki, Int. J. Appl. Glass Sci. **4**, 283 (2013).
[8] J. J. Neeway, S. N. Kerisit, J. Liu, J. Zhang, Z. Zhu, B. Joseph, R. Joseph, and V. Ryan, J. Phys. Chem. C **120**, 9374 (2016).
[9] O. L. Anderson and D. A. Stuart, J. Am. Ceram. Soc. **37**, 573 (1954).
[10] J. Kawamura, R. Asayama, N. Kuwata, and O. Kamishima, Phys. Solid State Ionics **81**, 193 (2006), https://www.researchgate.net/publication/280860465_Ionic_Transport_in_Glass_and_Polymer_Hierarchical_Structure_and_Dynamics.
[11] M. Holz, S. R. Heil, and A. Sacco, Phys. Chem. Chem. Phys. **2**, 4740 (2000).
[12] W. Meyer and H. Neldel, Z. Tech. Phys. (Leipzig) **18**, 588 (1937).
[13] N. Chandel and N. Mehta, J. Mater. Sci. **47**, 6693 (2012).
[14] Y. Gao, N. Li, Y. Wu, W. Yang, and S.-H Bo, Adv. Energy Mater. **11**, 2100325 (2021).
[15] R. Griesen, C. Boelsma, H. Schreuders, C. P. Broedersz, R. Gremaud, and B. Dam, ChemPhysChem **21**, 1632 (2020).
[16] G. J. Dienes, J. Appl. Phys. **21**, 1189 (1950).
[17] E. M. Njiokep, A. W. Imre, and H. Mehrer, J. Non-Cryst. Solids **354**, 355 (2008).
[18] R. A. Denny, D. R. Reichman, and J. P. Bouchaud, Phys. Rev. Lett. **90**, 025503 (2003).
[19] N. Takamure, A. Kondyurin, and D. R. McKenzie, J. Appl. Phys. **125**, 175104 (2019).
[20] D. Fragiadakis and P. Pissis, J. Non-Cryst. Solids **353**, 4344 (2007).
[21] M. P. F. Graça, M. G. Ferreira da Silva, A. S. B. Sombra, and M. A. Valente, J. Non-Cryst. Solids **353**, 4390 (2007).
[22] D. K. Burghate, V. S. Deogaonkar, S. B. Sawarkar, S. P. Yawale, and S. V. Pakade, Bull. Mater. Sci. **26**, 267 (2003).

[23] N. M. Johnson and D. J. Bartelink, J. Appl. Phys. **50**, 4828 (1979).
[24] F. Scholz, J. M. Hwang, and D. K. Schroder, Solid State Electron. **31**, 205 (1988).
[25] A. Das, V. A. Singh, and D. V. Lang, Semicond. Sci. Technol. **3**, 1177 (1988).
[26] W. Shockley, J. Appl. Phys. **9**, 635 (1938).
[27] R. H. Doremus, J. Phys. Chem. **68**, 2212 (1964).
[28] A. Einstein, Ann. Phys. (Berlin) **322**, 8549 (1905).
[29] M. Schafer and K.-M. Weitzel, Mater. Today Phys. **5**, 12 (2018).
[30] J. Martin, S. Mehrwald, M. Schafer, T. Kramer, C. Jooss, and K.-M. Weitzel, Electrochim. Acta **191**, 616 (2016).
[31] A. Yelon and B. Movaghar, Phys. Rev. Lett. **65**, 618 (1990).
[32] A. Yelon, B. Movaghar, and R. S. Crandall, Rep. Prog. Phys. **69**, 1145 (2006).
[33] S. Muy, J. C. Bachman, H.-H. Chang, L. Giordano, F. Maglia, S. Lupart, P. Lamp, W. G. Zeier, and Y. Shao-Horn, Chem. Mater. **30**, 5573 (2018).
[34] T. Yano, K. Azegami, S. Shibata, and M. Yamane, J. Non-Cryst. Solids **222**, 94 (1997).
[35] See Supplemental Material at http://link.aps.org/supplemental/10.1103/PhysRevLett.129.175901 for activation profiles for onsets of ion motion from TRIS results, depth profiles of doped soda-lime glass samples before and after TRIS, and comparison of Meyer-Neldel temperatures with other materials, which includes Refs. [36–39].
[36] J. C. Coleman, J. Miller, P. Close, W. B. Silverman, H. H. Holscher, F. R. Bacon, and C. L. Babcock, J. Am. Ceram. Soc. **27**, 221 (1944).
[37] M. H. Krohn, J. R. Hellmann, B. Mahieu, and C. G. Pantano, J. Non-Cryst. Solids **351**, 455 (2005).
[38] S. C. Agarwal, Bull. Mater. Sci. **19**, 39 (1996).
[39] H. Stohr and W. Klemm, Z. Anorg. Allg. Chem. **241**, 305 (1939).
[40] C. McLaren, B. Roling, R. Raj, and H. Jain, J. Non-Cryst. Solids **471**, 384 (2017).
[41] Y. L. Khait, R. Beserman, D. Shaw, and K. Dettmer, Phys. Rev. B **50**, 14893 (1994).
[42] R. Metselaar and G. Oversluizen, J. Solid State Chem. **55**, 320 (1984).
[43] S. K. Sharma and F. Faupel, J. Mater. Res. **14**, 3200 (1999).
[44] S. K. Sharma, S. B. Kuldeep, and A. K. Jain, J. Mater. Res. **4**, 603 (1989).
[45] U. Geyer, S. Schneider, W. L. Johnson, Y. Qiu, T. A. Tombrello, and M.-P. Macht, Phys. Rev. Lett. **75**, 2364 (1995).
[46] P. Fielitz, M. P. Macht, V. Naundorf, and G. Frohberg, J. Non-Cryst. Solids **250**, 674 (1999).
[47] K. Knorr, M. P. Macht, K. Freitag, and H. Mehrer, J. Non-Cryst. Solids **250**, 669 (1999).
[48] A. Sharma, N. Mehta, and A. Kumar, J. Alloys Compd. **509**, 3468 (2011).
[49] W. B. Jackson, Phys. Rev. B **38**, 3595(R) (1988).